Arab J Sci Eng (2016) 41:2731–2750
DOI 10.1007/s13369-016-2183-6

RESEARCH ARTICLE - PETROLEUM ENGINEERING

Characterizing the Role of Clay and Silica Nanoparticles in Enhanced Heavy Oil Recovery During Polymer Flooding

Seyyed Shahram Khalilinezhad[1] · Goshtasp Cheraghian[2] · Mohammad Saber Karambeigi[3] · Hamid Tabatabaee[4] · Emad Roayaei[3]

Received: 28 October 2015 / Accepted: 2 May 2016 / Published online: 18 May 2016
© King Fahd University of Petroleum & Minerals 2016

Abstract Polymer flooding as one of the most effective methods for enhancing oil recovery has a significant effect on tertiary production of reservoirs with poor vertical sweep efficiencies and those which are extremely heterogeneous. Water-soluble polymers are used to both increase the viscosity of water and decrease the mobility ratio of the displaced and displacing fluids. However, due to high amount of polymer adsorption, presence of divalent cations and mechanical degradation, polymer molecules may lose their properties. Hence it is necessary to further improve the displacement effectiveness of polymer flooding. Despite the fact that several ways have been suggested to enhance the performance of polymer flooding, application of nanoparticles in the improvement of rheological properties of the polymer solution used in enhanced oil recovery has not been reported previously and is still an ongoing subject. This paper investigates the effects of nanoparticles on flow behavior of polymer solution in porous media by employing both experimental studies and numerical simulations. The simulation model first is validated against well-controlled laboratory experiment to have reliable predictions of the full-field implementations. The results show that the amount of polymer adsorption and viscosity of polymer solution will improve when the clay or silica nanoparticles is present in the injectant, and accordingly, the cumulative oil recovery and breakthrough time will be bettered. The result of sensitivity analysis demonstrates that polymer molecules are more degradable during polymer flooding compared to nanoparticles-assisted polymer flooding. Based on the validated model, 3D simulations of nanoparticles-assisted polymer field pilot were performed and the results revealed that the cumulative oil recovery, water cut and breakthrough time will improve when the injectant has some dispersed nanoparticles.

Keywords Polymer flooding · Silica nanoparticles · UTCHEM

Abbreviations

SEM	Scanning electron microscopy
PV	Pore volume
TDS	Total dissolved solids
UTCHEM	The University of Texas Chemical Compositional simulator
3D	Three-dimensional

List of symbols

AP_1	Matching parameter for UTCHEM polymer viscosity model
AP_2	Matching parameter for UTCHEM polymer viscosity model
AP_3	Matching parameter for UTCHEM polymer viscosity model
AD41	Polymer adsorption parameter in UTCHEM
AD42	Polymer adsorption parameter in UTCHEM
B4D	Polymer adsorption parameter in UTCHEM
GAMMAC	UTCHEM parameter in shear rate dependence of polymer viscosity model

✉ Seyyed Shahram Khalilinezhad
Sh.khalilinezhad.srbiau@gmail.com

[1] Department of Petroleum Engineering, Quchan Branch, Islamic Azad University, Quchan, Iran

[2] Young Researchers and Elite Club, Omidieh Branch, Islamic Azad University, Omidieh, Iran

[3] IOR Research Institute, National Iranian Oil Company (NIOC), Tehran, Iran

[4] Department of Computer Engineering, Quchan Branch, Islamic Azad University, Quchan, Iran

POWN Parameter for shear rate dependence of polymer viscosity in UTCHEM
SSLOPE Parameter for salinity dependence of polymer viscosity in UTCHEM

1 Introduction

Production of the reservoirs containing medium to high oil viscosity plays a significant role in the petroleum industry due to the increasing demand for crude oil. Considering the distinctive characteristics of heavy oil resources, the production of such reservoirs meets some serious challenges [1]; therefore, enhanced oil recovery (EOR) methods are essential in order to maximize the cumulative production. Thermal EOR and chemical enhanced oil recovery (CEOR) methods have been suggested to enhance the cumulative oil recovery from heavy oil reservoirs [2–7]; however, the application of thermal methods such as steam flooding and in-situ combustion is strictly limited owing to their technical uncertainty [8–10].

CEOR methods such as polymer flooding, alkaline flooding and alkaline-surfactant-polymer (ASP) flooding are employed to improve the production of medium to heavy oil reservoirs, and there is an extensive body of literature on the application of CEOR methods to enhance heavy oil recovery [11–17]. Among different chemical flooding methods, polymer flooding is one of the most effective ways known to increase oil production. Particularly, the effect of polymer flooding on oil recovery is more significant when the reservoir has a high viscous crude oil or is heterogeneous. For such reservoirs, polymer flooding is a useful method to increase the volumetric sweep efficiency by improving the mobility ratio of displaced and displacing fluids [18–22]. However, due to high amount of polymer adsorption, presence of divalent cations and mechanical degradation, polymer flooding may become ineffective [23,24]. Hence it is necessary to further improve the displacement effectiveness of polymer flooding and to take account of the use of new applicable materials like nanoparticles in EOR; some studies have stated the role of them in CEOR methods [25–31].

Hendraningrat et al. [32] studied the effect of nanofluid on enhanced oil recovery in low- to high-permeability sandstones. They observed that interfacial tension (IFT) decreased when hydrophilic nanoparticles were introduced to brine. They also observed that the higher the concentration of nanofluid, the more the impairment of porosity and permeability in sandstone core plugs. Mohajeri et al. [33] showed that the presence of nanoparticles in surfactant solution increases oil recovery significantly. This enhancement for cationic surfactants is greater than anionic surfactants. In addition, adding nanoparticles to the surfactant solution leads to flow character modification from Newtonian to non-Newtonian.

Maghzi et al. [34] reported new experimental results of the effect of silica nanoparticles on heavy oil recovery during polymer flooding and concluded that ion–dipole interaction between cations and silica increases the viscosity of nanosuspension by increasing silica nanoparticles concentration. Therefore, oil recovery improves during flooding test by increasing the silica nanoparticles concentration. Other studies investigated the effect of nanoparticles on rock surface wettability during water flooding and polymer flooding [35,36]. Their results showed that silica nanoparticles can make the rock surface strongly water-wet, especially during water flooding and also when polymer concentration is low during polymer flooding. Cheraghian et al. [30] and Khalilinezhad et al. [27] studied the effect of silica and clay nanoparticles on the amount of polymer adsorption. They showed that silica and clay nanoparticles can reduce the amount of polymer adsorption onto the rock surface.

Despite conducting some experimental observations to investigate the effect of dispersed clay and silica nanoparticles on oil recovery during polymer flooding, there is lack of experimental and simulation studies. In addition, in the best of our knowledge this is the first time that the chemical compositional simulator is employed for studying CEOR methods using nanofluids. This paper examines the effects of dispersed nanoparticles on flow behavior of polymer solution in porous media by performing both experimental and simulation studies. Core scale simulations of polymer flood and nanoparticles-assisted polymer (NAP) flood are performed, and sensitivity analysis with respect to divalent cations concentration during NAP flood is carried out. Based on the validated model, 3D simulations of NAP field pilot were conducted and the results were compared to the conventional polymer flood.

2 Description of Reservoir Simulator

The reservoir simulator used in this work was a three-dimensional, multiphase, multicomponent chemical flooding simulator called UTCHEM and developed in the *Center for Petroleum and Geosystems Engineering at the University of Texas at Austin* [37–42]. UTCHEM uses a solution scheme analogous to implicit pressure, explicit saturation. The simulator has the option to simulate several chemical species such as water, oil, surfactant, polymer, cations, anions and tracers. Physical and chemical phenomena such as surfactant phase behavior, three-phase relative permeability, capillary phase trapping, shear-thinning polymer viscosity, polymer permeability reduction, cation exchange, tracer partitioning, chemical reactions, adsorption, gel reactions and temperature-dependent phase behavior are modeled. Figure 1 shows the UTCHEM calculation flowchart. Particularly, UTCHEM shows better results [43] for simulation of

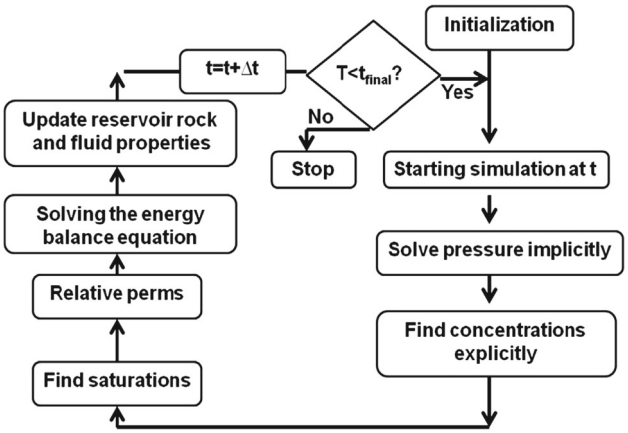

Fig. 1 UTCHEM calculation flowchart [44]

Table 1 Chemical composition of bentonite

Formula	wt%
L.O.I	13.2
Na_2O	2.04
MgO	2.22
Al_2O_3	14.59
SiO_2	61.03
SO_2	0.37
Cl	0.46
K_2O	0.76
CaO	0.77
TiO_2	0.22
Fe_2O_3	2.09
BaO	0.11

polymer flood owing to the fact that polymer adsorption and subsequent reduction in polymer concentration are modeled in UTCHEM. Other noteworthy feature of this simulator includes its specialized ability to model laboratory-scale experiments. It should be mentioned that the phase displacements during chemical flooding are displayed, in this paper, by Kraken software (http://www.esss.com.br/Kraken/).

3 Material and Methods

3.1 Materials

The polymers used in this study are all commercially available and completely water soluble. In particular, polyacrylamide (PAM) polymer chemically similar to acrylamide from Beijing Hengju Company, with an average molecular weight (MW) of 12.0×10^6, was tested. Sodium bentonite with a mesh size of 200 and particles size less than 75 nm was used. The bentonite is produced in Iran and amended with the chemicals shown in Table 1. Oxford-ED2000 XRF and GC-2550TG (Teif Gostar Faraz Company, Iran) were used for all chemical analyses. Fumed nanosilica (Aerosil A300) was purchased from Degussa. Specific surface area of Aerosil is 300 m^2/g with an average primary particle size of 7 nm, pH of 3.7–4.7 and SiO_2 content of 99.8 wt%. The SEM images of the prepared clay and SiO_2 nanoparticles are shown in Fig. 2. It should be noticed that the most important feature of lipophobic and hydrophilic nanoparticles is that they can easily be dispersed in water-based fluids such as brine [32].

In this study, two samples were required: One solution was the dispersed clay nanoparticles in polymer (DCNP) solution, and the other one was dispersed silica nanoparticles in polymer (DSNP) solution. To prepare DCNP solution, 0.9 wt% clay nanoparticles were dispersed in the distilled water by means of ultrasonic probe for 1 h; then, 3150 ppm solid PAM was added to the prepared solution and was stirred for 48 h by a simple homogenizer. Concentration of solid polymer in all aqueous solutions was 3150 ppm. The usual range of polymer concentration in polymer flooding projects is 1000–5000 ppm [45]. To prepare DSNP solution, 0.45 wt% silica nanoparticles were dispersed in the distilled water by means of ultrasonic probe for 1 h; then, 3150 ppm solid PAM was added to the prepared solution and was stirred for 48 h by a simple homogenizer. To evaluate the effect of salt concentration on the performance of the prepared solutions, the water salinity of one of the Iranian oil reservoirs was used. Composition of salt is shown in Table 2. Finally, desirable amount of salt (20,000 ppm) was dissolved in both DSNP and DCNP solutions using a simple homogenizer. After preparation of samples, for assurance of the homogeneity and stability of prepared solutions, the solutions were placed for 10 days in a closed transparent bottle away from degrading factors such as light and heat. Following this, the DSNP and DCNP solutions were examined and no precipitation and significant color alteration in samples were detected indicating the good stability for both samples. Figure 3 shows the prepared DCNP and DSNP solutions at different conditions.

In this study, sandstone sample of one of Iranian oil reservoirs was used. Permeability and porosity of sandstone rock were 5.5 md and 21 %, respectively. Figure 4 shows the sandstone sample used in this study.

3.2 Experimental Procedure for Determining Simulator Parameters for Polymer Properties

The common polymer data to model the flow of polymer solution through porous media consist of: polymer viscosity as a function of shear rate, polymer concentration, salinity and permeability reduction factor as a function of permeability. Another important parameter is polymer adsorption.

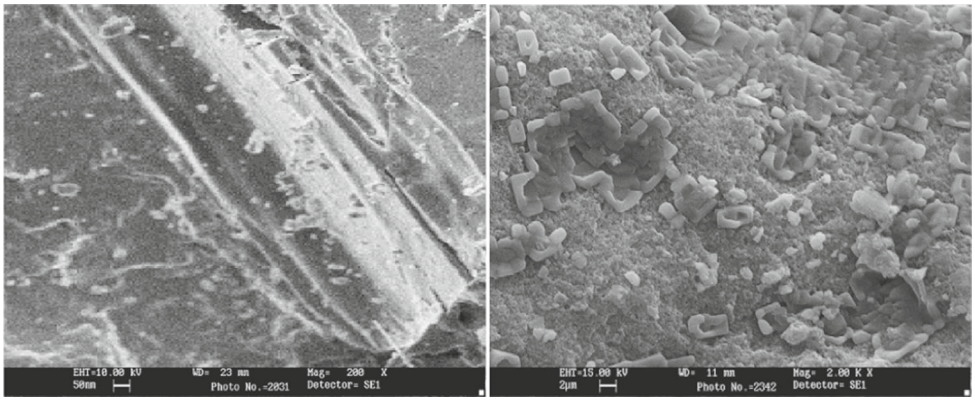

Fig. 2 SEM images of the nanoparticles, *left* clay nanoparticles, *right* silica nanoparticles

Table 2 Composition of salt

Composition	Weight %
NaCl	1.71
NA_2SO_3	0.01
$CaCl_2$	0.32
$MgCl_2 \cdot 6H_2O$	0.09
Na_2HCO_3	0.02

This section will present the methods used for obtaining the UTCHEM parameters for the prepared solutions properties.

One of the most important parameters for polymer solution is the modeling is the shear dependence of polymer viscosity. The polymer solution exhibits non-Newtonian behavior, and its viscosity is a function of the shear rate. The viscosity of the prepared solutions was measured using a DV-III ULTRA+
Brookfield rheometer. The principle of operation of the DV-III Ultra is to drive a spindle (which is immersed in the test fluid) through a calibrated spring. The viscous drag of the fluid against the spindle is measured by the spring deflection. Spring deflection is measured with a rotary transducer. The viscosity measurement range of the DV-III Ultra (in centipoise or cP) is determined by the rotational speed of the spindle, the size and shape of the spindle, the container the spindle is rotating in and the full-scale torque of the calibrated spring [46]. In each measurement, the shear rate was changed, and the effect of this change on the viscosity of the prepared solutions was measured. The values of these viscosities were matched using polymer shear-thinning model of UTCHEM [40].

Another important property of a polymer solution is its ability to increase the solution viscosity. As the polymer concentration increases, the amount of solution viscosity will also increase. For both DSNP and DCNP solutions, polymer viscosities at different polymer concentrations (at a fixed salinity, shear rate and nanoparticles concentration) were measured using DV-III ULTRA+Brookfield rheometer.

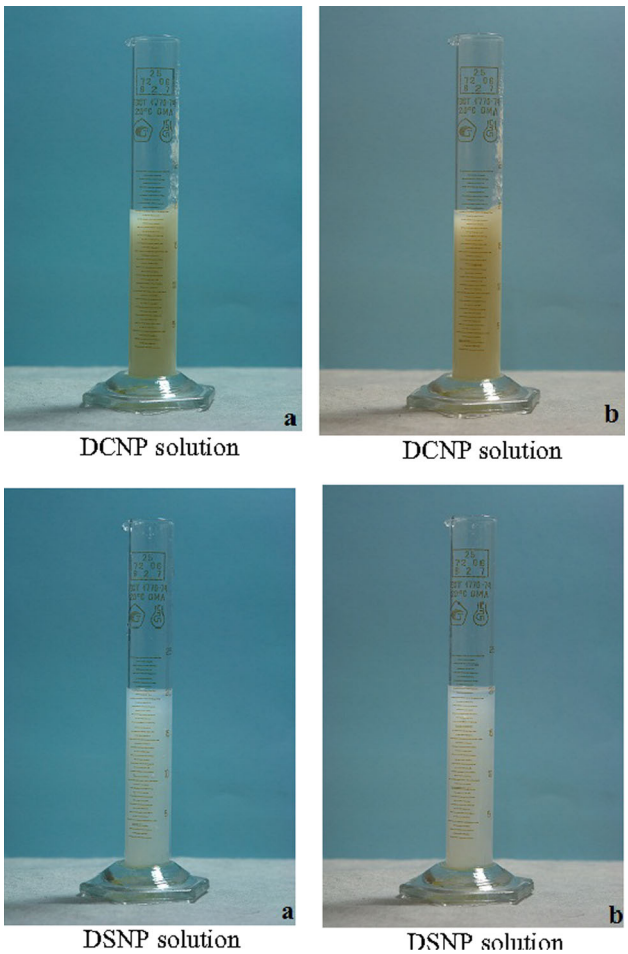

Fig. 3 Stability tests, **a** immediately after preparation, **b** after 10 days of preparation

Another significant parameter of polymer properties is polymer adsorption. The amount of polymer adsorption is one of the most important properties which can determine the efficiency of polymer flooding in oil recovery. Adsorption and retention may be defined as the interaction between the polymer molecules and the porous medium which leads polymer to be retained or adsorbed. The adsorption and reten-

Fig. 4 Sandstone sample

Table 3 Core and fluid properties

Length (cm)	29.08
Diameter (cm)	4.93
Porosity	0.18
Brine permeability (mD)	172
Oil viscosity (cP)	300
Water viscosity (cP)	0.95

tion of polymer will affect both polymer and porous medium properties. Static adsorption experiments were performed to evaluate the adsorption of DSNP and DCNP solutions onto the sandstone surface. These tests were conducted at room temperature by adding degassed sand to both solutions and stirring until adsorption was complete; then, the amount of adsorbed polymer was calculated. The experimental details of the adsorption tests can be found elsewhere [47]. This procedure was repeated for different polymer concentrations, while no change had been made to the amount of salinity and nanoparticle concentration in both solutions.

3.3 Core Flood Experiments

Ehrenfried [48] conducted several core floods to investigate the effect of polymer injection on viscous oil recovery from sandstone core plugs; the core flood of our interest is one of his experiments. A highly permeable sandstone core with the length of 29.08 cm and a diameter of 4.93 cm was used. A 1.5-PVs polymer slug was injected containing 1500 ppm hydrolyzed polaycarylamide (HPAM) solution in water with 1.5 % NaCl. The core flood was conducted at flow rate of 0.1 ml/min, and the oil recovery was about 51 %. The detail of experimental procedure can be found elsewhere [48]. The main rock and fluid properties are listed in Table 3.

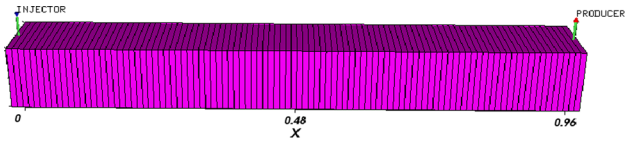

Fig. 5 Simulation model for core flood experiment

3.4 Numerical Simulation

The UTCHEM simulator was used to history match average oil saturation data. The numerical model uses 100 grid blocks to simulate the behavior of the core (Fig. 5). The rheological behavior of HPAM (Flopaam 3630S) solution is based on the laboratory data provided by Mohammadi [49]. Additionally, the following is a list of assumed matching parameters for simulation of polymer flood:

i Relative permeability parameters
ii Capillary pressure parameters
iii Capillary desaturation parameters

Clearly, the oil recovery is related particularly to the properties of relative permeability curves. In relative permeability curves, for each phase, three parameters can be tuned to achieve the best values based on the history match of the average oil saturation. They are 1) residual saturation, 2) relative permeability endpoint, 3) relative permeability exponent.

UTCHEM uses Corey-type relative permeability for both oil and water phases. A few relative permeability exponents and endpoints for both oil and water phases were tested in an acceptable range of apparatus measurement to select the best results based on history match of average oil saturation data.

4 Results and Discussion

4.1 Rheological Experiments

The rheological behavior of both DCNP and DSNP solutions is depicted in Fig. 6. Results from the rheological analysis show that the DCNP and DSNP solutions all exhibit bulk shear-thinning behavior (Fig. 6). In addition, it can be observed that DSNP solution has a higher viscosity compared to DCNP solution; moreover, DSNP solution is less sensitive to the shear rate variation. These results indicate that DSNP and DCNP solutions have a higher viscosity compared to the conventional polymer solutions such as HPAM solution. In fact, adding silica nanoparticles or clay nanoparticles to the polymer solution increases the solution viscosity. According to the Maghzi et al. [34], silica nanoparticles have the ability to prevent polymer degradation in the presence of salt. Generally, when nanoparticles are dispersed in PAM solution,

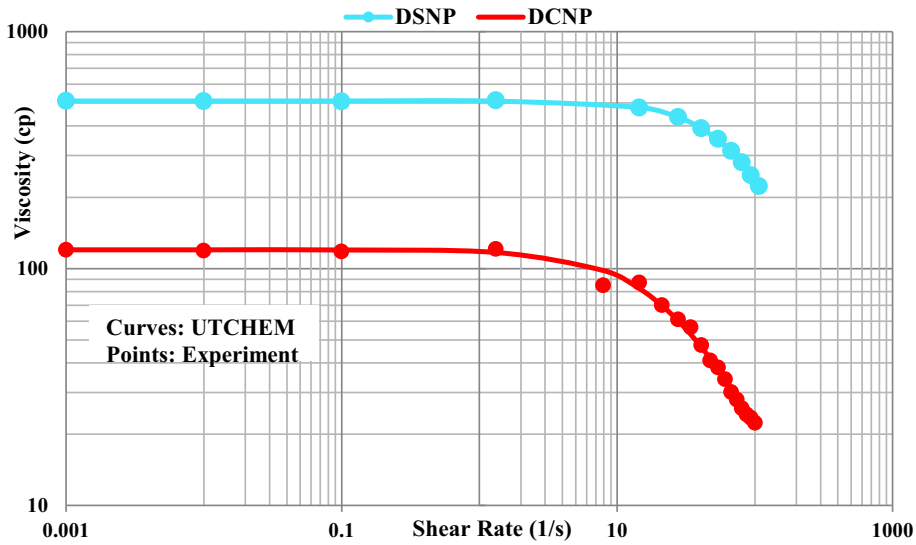

Fig. 6 Viscosity of different solutions as a function of shear rate

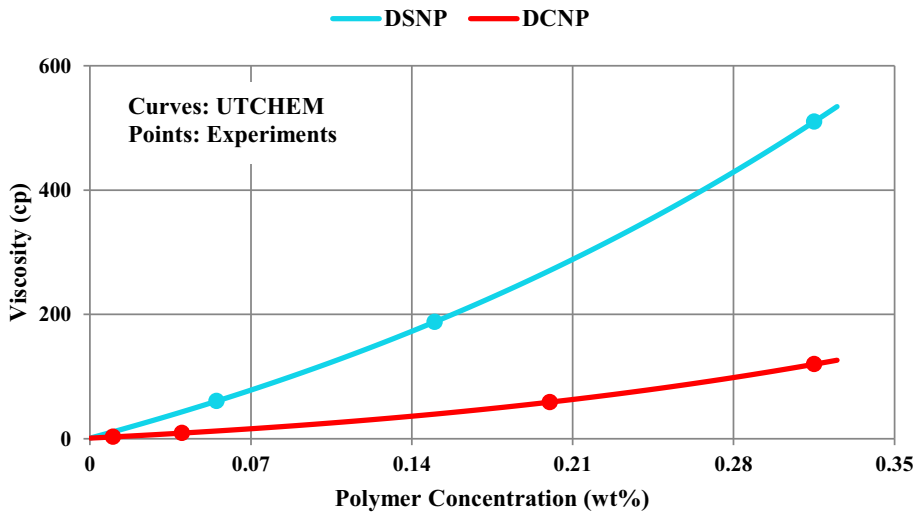

Fig. 7 Viscosity of different solutions as a function of polymer concentration

nanoparticles and polymer molecules will be in competition for attracting the cations. Thus, ion–dipole interaction between the nanoparticles and cations decreases the degradation of polymer molecules; therefore, the viscosity of solution increases.

One of the most important properties of a polymer solution is its ability to increase the solution viscosity. For both DSNP and DCNP solutions, polymer viscosities at different polymer concentrations (at a fixed salinity and nanoparticles concentration) were measured and values were matched (Fig. 7) using UTCHEM polymer model [40]. According to the results, viscosity of DSNP solution is strongly dependent on polymer concentration and as the polymer concentration increases, the solution viscosity increases dramatically; however, the DCNP solution is not as strongly dependent on polymer concentration as DSNP solution is.

Fig. 8 Sandstone sample used in static adsorption test of DSNP solution

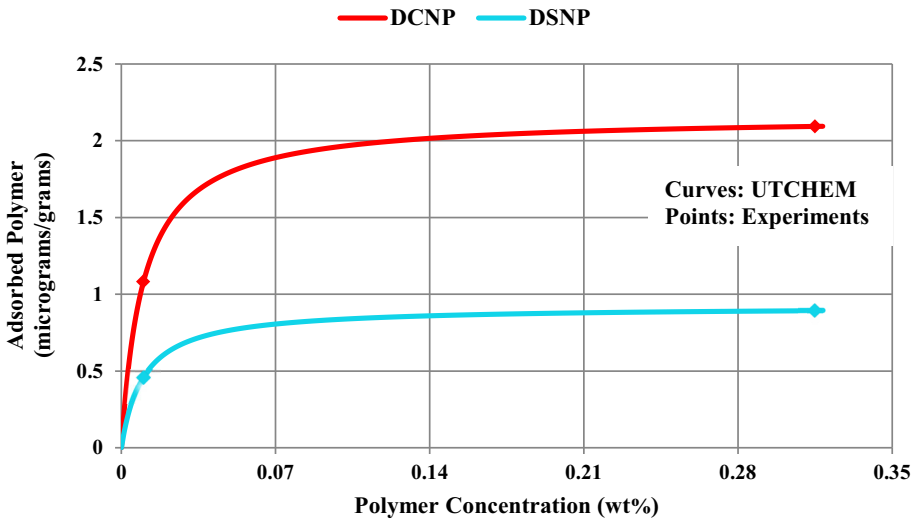

Fig. 9 Comparison of laboratory data of polymer adsorption with UTCHEM model for different solutions

Figure 8 shows the amount of adsorbed polymer of DSNP solution onto the rock sample, and Fig. 9 depicts the amount of polymer adsorption as a function of polymer concentration for both DSNP and DCNP solutions. The adsorption values were matched using polymer adsorption model in UTCHEM [40], and Fig. 9 also delineates the matched graph. According to the experimental observations, the amount of polymer adsorption is less for DSNP solution than DCNP solution. These results declare that dispersed nanoparticles in polymer (DNP) solutions have an ultra-low adsorption of polymer compared to the conventional polymer solutions. Previous studies demonstrate that biopolymers such as xanthan gum have a less adsorption compared to synthetic polymers such as PAM polymer [50]. PAM polymers are adsorbed strongly on mineral surfaces, and recently, the polymers are partially hydrolyzed to reduce the amount of adsorption by reacting polyacrylamide with a base, such as sodium or potassium hydroxide or sodium carbonate [51]. Consequently, adsorption behavior of DNP solutions is more similar to the biopolymers. Finally, the results demonstrate that dispersed nanoparticles can improve the adsorption behavior of PAM solution.

Our experimental observations show that the amount of polymer adsorption for both DSNP and DCNP solutions is in complete agreement with experimental results published by Maghzi et al. [35] and Khalilinezhad et al. [27]. They concluded that the amount of polymer adsorption will decrease when nanoparticles are added to polymer solution.

Other essential properties of the prepared solutions, such as permeability reduction factor, and dependency of polymer viscosity on salinity for simulation of both DSNP and DCNP floods were calculated experimentally, and they are listed in Table 4.

Table 4 UTCHEM input parameters used in the simulation of DSNP flood and DCNP flood

UTCHEM parameter	DCNP solution	DSNP solution
SSLOPE	−0.32	−1
AP1	120	310
AP2	230	430
AP3	510	570
GAMMAC	4	4
GAMHF	27.5	90
POWN	2.2	2.5
AD41	0.192	0.08
AD42	0.0682	0.0345
B4D	100	100

4.2 Validation of Simulation Model

Figure 10 depicts the experimental results of HPAM flood. The results from laboratory [48] show that oil saturation starts at around 0.76. It decreases quickly at the beginning and then gradually declines to 0.37 at 1.5 PVs. According to the experimental data, cumulative oil recovery was measured about 51.9 % of original oil in-place (OOIP).

The simulation results show that oil saturation starts out at 0.76 and gradually declines to 0.369. The simulated oil cut starts relatively high and then quickly declines to about 0.2 at 1.5 PVs. Cumulative oil recovery increases to about 43 % at 0.53 PV and then assumes a gentler slope until it reaches to about 52 % at 1.5 PVs. The agreement between simulation results compared with the experimental data including

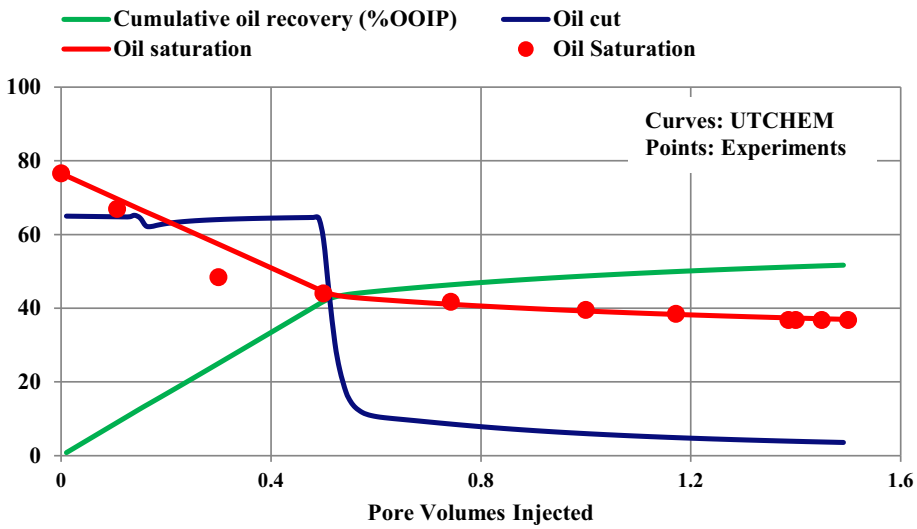

Fig. 10 Average oil saturation match, oil cut and cumulative oil recovery for the HPAM flood

Table 5 Tuned relative permeability and capillary pressure curves

Relative permeability endpoint	Water = 0.14 Oil = 0.90
Relative permeability exponent	Water = 3.1 Oil = 2.4
Residual saturations	Water = 0.11 Oil = 0.26
Capillary pressure endpoint	0
Capillary pressure exponent	2

saturation profile is generally good. Figure 10 depicts the comparison of the results as well as cumulative oil recovery and oil cut results. Table 5 shows the tuned capillary pressure and relative permeability curve parameters. In addition, Fig. 11 shows the tuned relative permeability curves for HPAM flood. Matching performance in this section indicates that the simulation model is reliable. This model can be taken into account as basis for further investigations. It was assumed that the flow behavior of both DCNP and DSNP solutions in porous media is similar to the HPAM solution. As a result, Fig. 11 also shows the tuned relative permeability curves for DCNP and DSNP floods from UTCHEM coreflood history match and their values are shown in Table 5.

4.3 Roles of Silica and Clay Nanoparticles on Oil Recovery

In this part, the roles of silica and clay nanoparticles on heavy oil recovery during polymer flooding will be investigated; therefore, the rheological properties already measured for DCNP and DSNP solutions are imported to the simulator. Moreover, the simulation results of HPAM flood are used as a base case in order to evaluate the performance of DCNP flood and DSNP flood, precisely. Based on the validated simulation model, the tuned parameters such as endpoints and exponents of relative permeability curves are employed for simulation of both DCNP and DSNP floods. It is assumed that these tuned parameters can represent the fluid flow through porous media during both DCNP and DSNP floods. The core and fluid properties used in the simulations can be found in Table 3. The initial oil saturation (So_i) for both simulation models is also the same as HPAM flood which is equal to 0.766.

Similar to the HPAM coreflood design, injection schemes for both DCNP and DSNP floods are defined in the simulation models. In the first simulation run, 1.5 PVs of clay nanoparticles suspension in polymer solution was injected containing 1500 ppm PAM polymer and 0.9 wt% clay nanoparticles dispersed in polymer solution with 13744 ppm salinity, and consequently, the effect of DCNP solution on heavy oil recovery was simulated. For the next simulation run, injection scheme for DSNP flood remains similar to the DCNP flood other than that there are no dispersed clay nanoparticles and polymer solution has 0.45 wt% dispersed silica nanoparticles. It should also be noted that the injection rate is constant for both of them and it is equal to 0.1 ml/min.

According to the simulation results which are depicted in Fig. 12, cumulative oil recovery for the case of DSNP flood is much higher than both DCNP and HPAM floods and it is about 65 % of OOIP. Both DSNP and DCNP floods improve heavy oil recovery compared to HPAM flood, while cumulative oil recovery for DCNP flood and HPAM flood is 59 % of OOIP and 51.5 % of OOIP, respectively. In addition, DSNP flood has a higher breakthrough time compared to other cases. In fact, the simulation results revealed that the advantage of conducting DSNP flood is an incremental oil recovery about 13.5 % of OOIP compared to the conventional HPAM flood. Accordingly, the average residual oil saturation

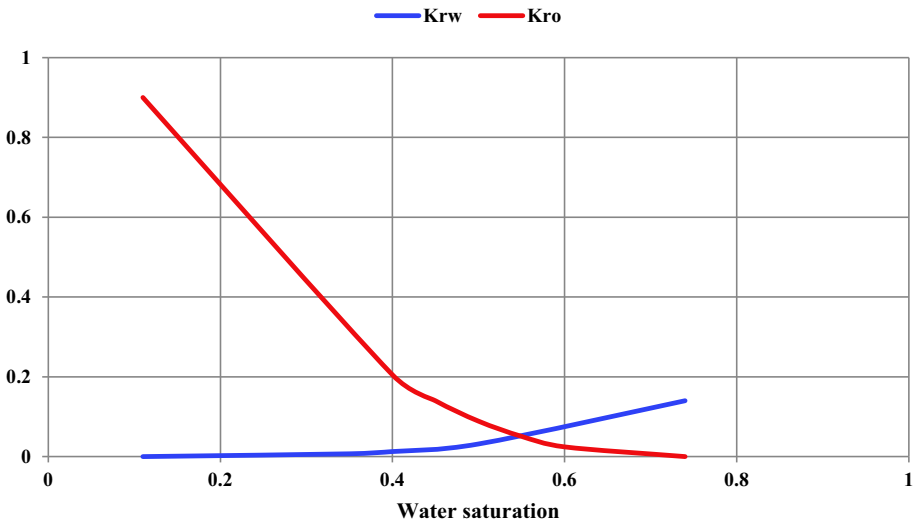

Fig. 11 Tuned relative permeability curves for simulations of HPAM, DCNP and DSNP floods

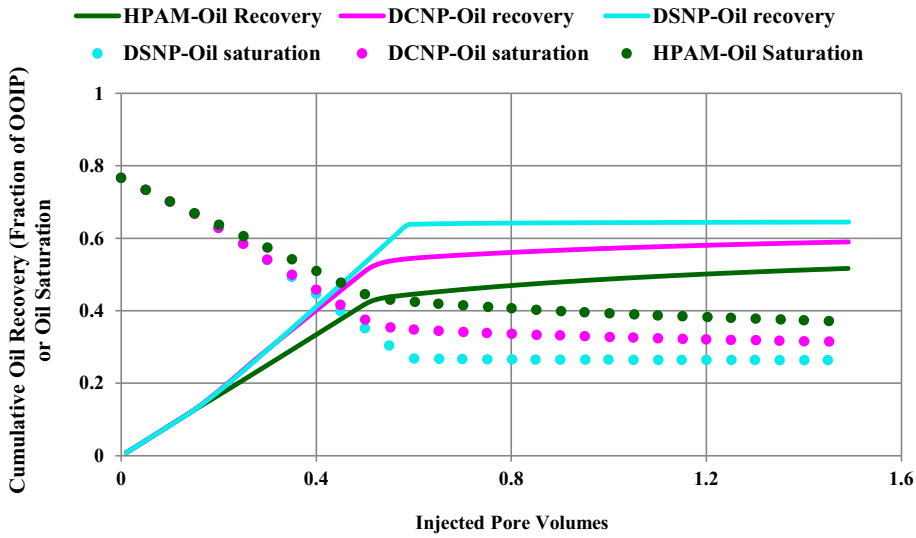

Fig. 12 Comparison of oil recoveries and average oil saturations for HPAM flood, DCNP flood and DSNP flood

for DSNP, DCNP and HPAM floods is 0.26, 0.31 and 0.37, respectively.

Figures 13, 14 and 15 show the distribution of oil saturation at the end of HPAM, DCNP and DSNP floods, respectively. These figures proclaim that the amount of residual oil saturation (So_r) is remarkably low particularly for DSNP flood in comparison with both HPAM and DCNP floods. The simulation results indicate that injection of DCNP solution or DSNP solution improves ultimate oil recovery and breakthrough time dramatically and this indicates a potential for EOR. We are seeking to find out some reasons for the effectiveness of DSNP and DCNP floods in the next part.

Polymer adsorption onto the rock surfaces has been an important issue in EOR applications. In fact, polymer adsorption can make a large negative impact on the performance of polymer flood; hence, the amount of polymer adsorption onto the rock surface should be reduced as much as possible. It is generally believed that sandstone formations are negatively

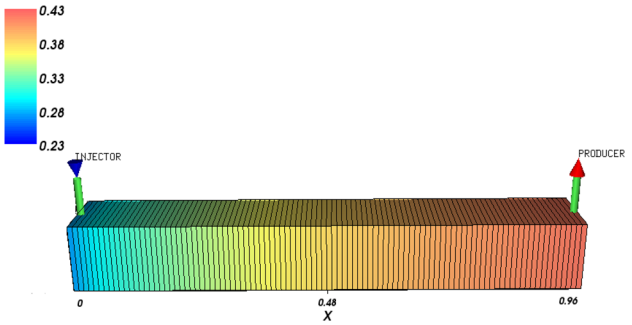

Fig. 13 Distribution of oil saturation at the end of HPAM flood

charged and carbonate formations are positively charged; therefore, polymer adsorption is dominated by electrostatic interactions between the charged groups that are present at the polymer/brine and rock/brine interfaces [52,53].

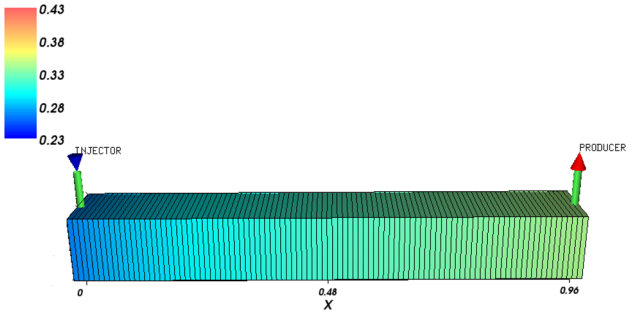

Fig. 14 Distribution of oil saturation at the end of DCNP flood

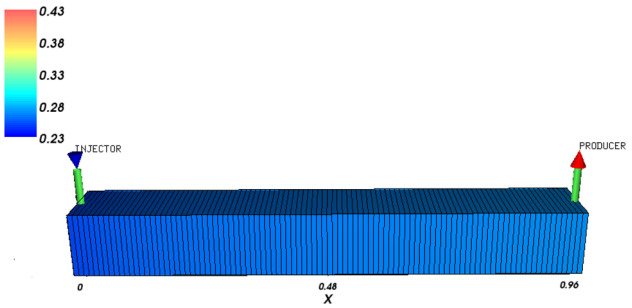

Fig. 15 Distribution of oil saturation at the end of DSNP flood

Based on the static adsorption measurements for DSNP and DCNP solutions depicted in Fig. 9 and common properties of HPAM solution, the simulation study regarding the effect of clay and silica nanoparticles on the performance of polymer flooding was carried out. According to the simulation results depicted in Fig. 16, the amount of polymer adsorption during DSNP and DCNP floods drastically declined compared to HPAM flood. These results are completely in agreement with our experimental observations. To the best of the authors' knowledge, there is no published work on the simulation study of NAP flooding and there is lack of simulation study concerning the effect of nanoparticles on the amount of polymer adsorption in the literature.

Considering the previous results [51], adsorption of PAM solution will decrease when polymer is partially hydrolyzed. Moreover, some studies investigated the effect of alkali on the amount of polymer adsorption and they showed that its effect on polymer and rock surface results in an enhancement of oil recovery by decreasing polymer adsorption and improving injectivity [54].

Our numerical simulation results and experimental observations also show that dispersed clay and silica nanoparticles reduce the amount of polymer adsorption, while the later has more effect on polymer adsorption. This is a significant finding in improvement of polymer properties used in CEOR methods for the researchers because several studies showed that the most conventional HPAM polymers reduced the permeability of the porous media through adsorption onto the rock surface and mechanical entrapment.

During DSNP and DCNP floods, complete adsorption of polymer onto the rock surface decreases and just a few of them can adsorb on surface in competition with silica or clay nanoparticles and oil.

Increasing the viscosity of the injectant is the most important reason to use polymers in EOR methods. This will reduce the mobility ratio and better mobilize the original oil with smooth profile. There are some issues about polymer flooding such as polymer good transport in porous media and shear stability which still can be considered as an open area of research. In addition, high salinity either by monovalent ion or by divalent ions will reduce polymer viscosity.

In this part, the aqueous phase viscosity profiles for three polymeric solutions will be compared. To put it more clearly, aqueous phase viscosity profiles for HPAM, DCNP and DSNP solutions between the injector and producer ports are examined. Based on the rheological properties of DSNP and DCNP solutions shown in Figs. 6 and 7, dispersing clay nanoparticles or silica nanoparticles improves the viscosity of polymer solution. Figure 17 shows the aqueous phase viscosity profiles for HPAM, DCNP and DSNP solutions at the end of HPAM, DCNP and DSNP floods, respectively. As the results show, the aqueous phase viscosity is dramatically high for the case of DSNP flood and now it is more favorable to push out viscous oil, while aqueous phase viscosity is relatively low for HPAM flood. These results indicate that dispersed clay and silica nanoparticles improve the aqueous phase viscosity which can affect oil recovery during polymer flooding. However, the feasibility of these new agents in terms of their injectivity should be investigated.

4.4 Salt Tolerance of Dispersed Nanoparticles in Polymer Solution

The existence of harsh conditions in an oil reservoir (e.g., high temperature, high pressure, chemical substances and bacteria in oil reservoirs) affects the rheological properties of polymer solutions [23]. These factors cause degradation of polymer molecules due to which the polymer viscosity decreases. UTCHEM simulator models polymer viscosity as a function of salinity and divalent cations (hardness) [40]. Based on our rheological experiments, the dependency of DCNP and DSNP solutions on salinity was measured and imported to the simulation models as an input. Hence in this part, the salinity of injectant changes and then the performance of DCNP and DSNP floods is investigated. Figure 18 shows that as the salinity of the injectant increases, the ultimate oil recovery decreases. In fact, increasing the amount of salinity has a severe impact on reduction of polymer viscosity. But, the effect of dispersed clay nanoparticles or dispersed silica nanoparticles on the performance of polymer flood is obvious. The negative effect of increasing salinity on the performance of DSNP in oil recovery is relatively negligi-

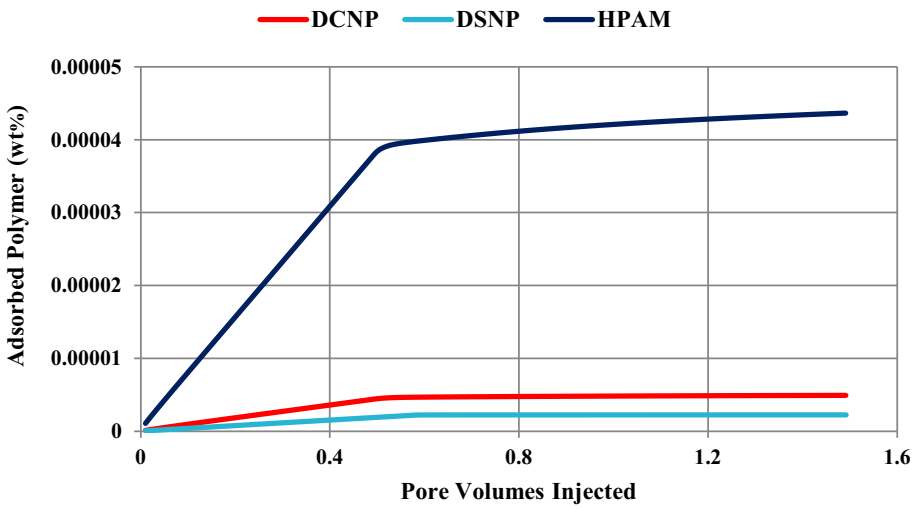

Fig. 16 Polymer adsorption versus pore volumes injected during DSNP flood, DCNP flood and HPAM flood

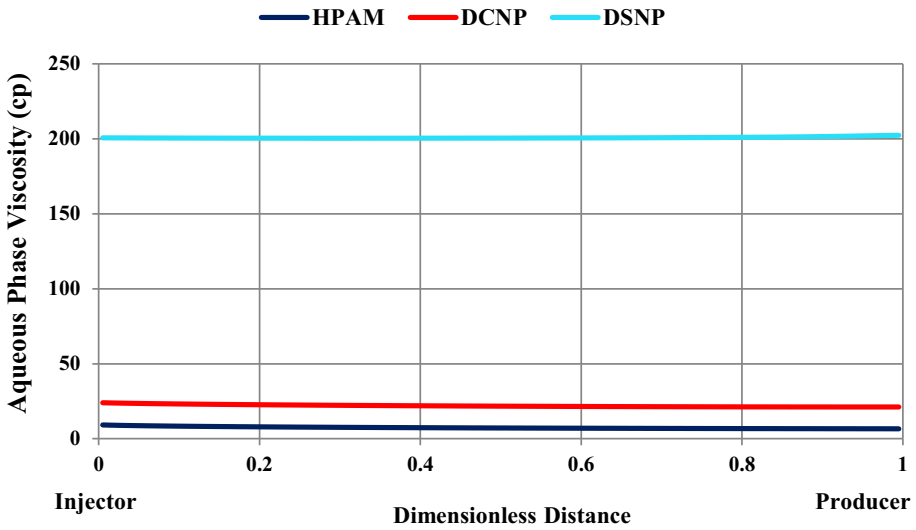

Fig. 17 Comparison of aqueous phase viscosity profiles after 1.6 injected PVs for different chemical slugs

ble. In addition, the behavior of DCNP solution to increase the salinity is similar to the DSNP solution but with a lesser extent. Moreover, some studies [36] showed that dispersed nanoparticles in water also increase the water viscosity. Their results demonstrated that dispersed nanoparticles have solely the ability to increase water viscosity.

4.5 Scale-Up Simulations

In this section, a 3D heterogeneous quarter of five-spot symmetry model with 15 × 15 × 10 grid blocks is used to track the impact of polymer flood and also NAP flood on oil recovery in tertiary-mode scenarios. Square grid blocks of size 50 × 50 ft^2 are used with relatively constant thickness of about 10 ft for the vertical layers. Injector and producer wells are completed over the whole reservoir thickness. The reservoir sand formation is characterized by high permeability, and porosity and a Dykstra–Parson (DP) coefficient of 0.61 are used to represent the field heterogeneity. Figure 19 shows the absolute permeability in x-direction and also wells configuration. Figure 20 shows the porosity distribution in the model. The reservoir is 4700 feet deep, 95° F. Reservoir crude is 17° API and with a viscosity of 300 cp at reservoir condition. The formation water is relatively fresh with salinity of approximately 13,744 ppm and a viscosity of 0.95 cp. There was no initial gas cap. Figure 21 shows the initial oil saturation distribution in the simulation model. The properties of this reservoir are summarized in Table 6. The model used Corey's exponents from Table 5 for HPAM, DCNP and DSNP floods. The initial oil in-place (IOIP) of the model was about 0.491 MMbbl, and the reservoir pore volume was about 0.581 MMbbl. The reservoir was first water flooded for about 1090 days (water cut of about 95 %). The water injection was performed at a rate of 800 barrels per day, and the production well was pressure constrained with bottom-hole pressure of 700 psi. The injector and producer wellbores had a radius equal to 0.3 ft and skin factor equal to zero.

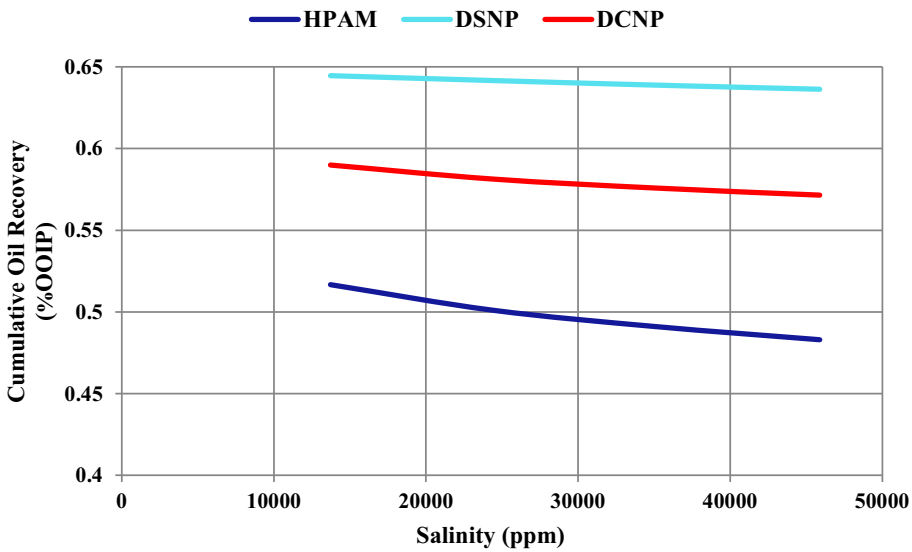

Fig. 18 Effect of salinity on oil recovery during flooding with different solutions

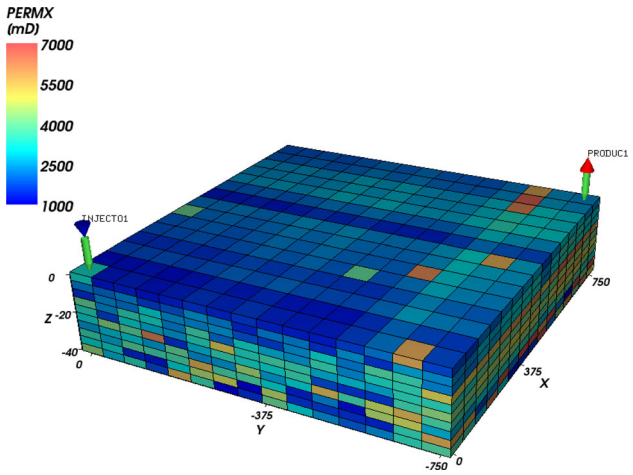

Fig. 19 Absolute permeability distribution in the x-direction for the 3D case

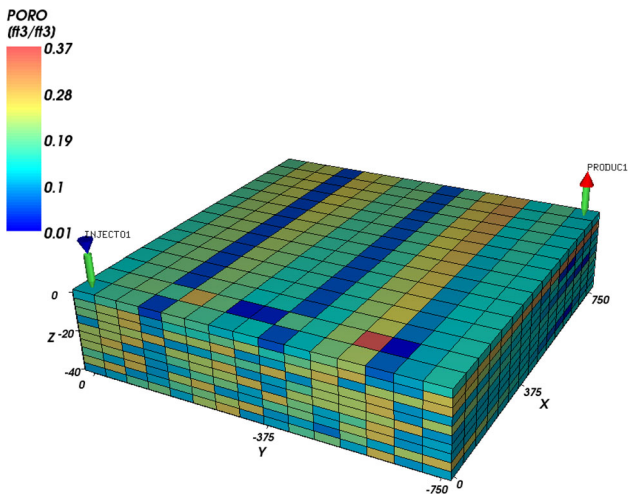

Fig. 20 Porosity distribution for the 3D case

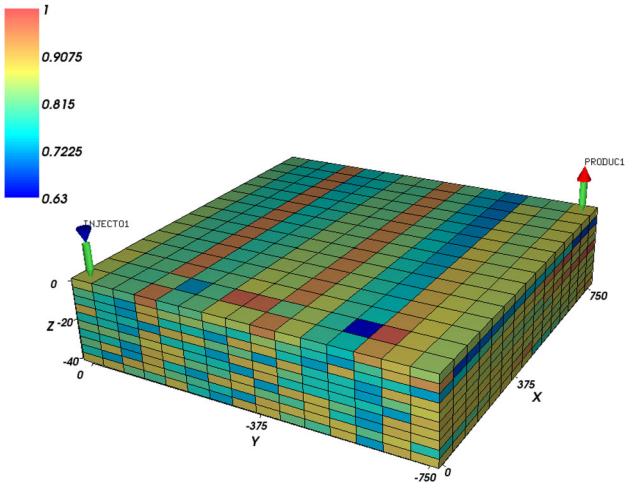

Fig. 21 Initial oil saturation distribution for the 3D case

Figure 22 shows the cumulative oil recovery, oil production rate and water cut during water flooding. At the beginning, although the injected water moves toward the highly permeable portions/layers of the reservoir, the oil production rate increases extremely slowly. At this time, the amount of water cut is relatively low and cumulative oil recovery is about 18 % of OOIP. After 100 days of water flood, the amount of water cut increases sharply and the oil production rate decreases. In other words, due to heterogeneous nature of the model and the undesirable mobility ratio between displaced and displacing fluids, water cones toward the production well and large pockets of bypassed oil still exist after the water flood. To put it more clearly, the high amount of model heterogeneity and unfavorable mobility ratio makes water flood ineffectual way to enhance heavy oil recovery. Figure 23 shows the remaining oil saturation at

the end of water flood. The simulation results show that the ultimate oil recovery factor is about 39 % of OOIP and the average oil saturation after water flooding is about 0.55. The reservoir condition after water flood is close to its economic limit and subject to abandonment. Furthermore, the reservoir has a high remaining oil saturation and low reservoir pressure. Consequently, it is a potential candidate for other EOR methods such as polymer flood.

The purpose of this part is to determine the ability of polymer and NAP floods on oil recovery, oil production rate and water cut in tertiary-mode scenarios. According to the simulation results of the water flood, reservoir has high remaining oil saturation due to unfavorable mobility ratio and low sweep efficiency. Generally, one of the most popular drawbacks of water flood is recognized to be its poor sweep efficiency when the reservoir is extremely heterogeneous or it has high viscous oil. Polymer flooding is one of the mobility control processes in which a low-mobility displacing agent is injected to increase the overall recovery efficiency. In this particular case, the target oil for polymer flooding is the bypassed viscous oil considering the unsatisfactory sweep efficiency of the water flood in this heterogeneous reservoir.

Simulation results of both DCNP and DSNP floods showed that dispersed clay nanoparticles or dispersed silica nanoparticles can improve the efficiency of polymer flood by decreasing polymer adsorption and increasing solution viscosity. Accordingly, simulation study of the effect of HPAM, DCNP and DSNP floods on oil recovery is carried out for a 3D heterogeneous reservoir. The purpose of this study is to evaluate the performance of each injectant on overall sweep efficiency. The resultant reservoir conditions after water flood are used as initial conditions for consequent polymer flood. For conventional HPAM flood, injection scheme included 1453 days or 1 PV polymer injection followed by 712 days or 0.5 PV water injection. The polymer slug included 1500 ppm HPAM polymer, and post-flush water flood salinity was around 13,744 ppm TDS which was the same as the polymer slug. Injection time and salinity of the injectant are the same as HPAM flood for two other cases, but 0.45 wt% silica nanoparticles were dispersed in the polymer solution for the case of DSNP flood. In the case of DCNP flood, 0.9 wt% clay nanoparticles were dispersed in polymer solution. Injection scheme is summarized in Table 7. Based on the experimental observations [55], dispersed nanoparticles prevent the thermal degradation of polymer molecules, so that they can improve the thermal stability of polymer solutions. Accordingly, the rheological data for HPAM, DCNP and DSNP solutions in reservoir condition are based on those presented in the last sections which were measured at laboratory condition.

Figure 24 shows the cumulative oil recovery versus injection days/pore volumes injected for HPAM, DCNP and DSNP floods. Simulation results declare that HPAM flood can improve cumulative oil recovery compared to the conven-

Table 6 Reservoir rock and fluid properties

Model physical dimension	750 ft × 750 ft ×40 ft
Depth	4700 ft
Porosity	Average = 0.145
Permeability	Average = 3280 md
K_v/K_h	0.05
Residual saturation	Oil = 0.26
	Water = 0.11
Corey-type relative permeability endpoint	Oil = 0.90
	Water = 0.14
Corey-type relative permeability exponent	Oil = 2.4
	Water = 3.1

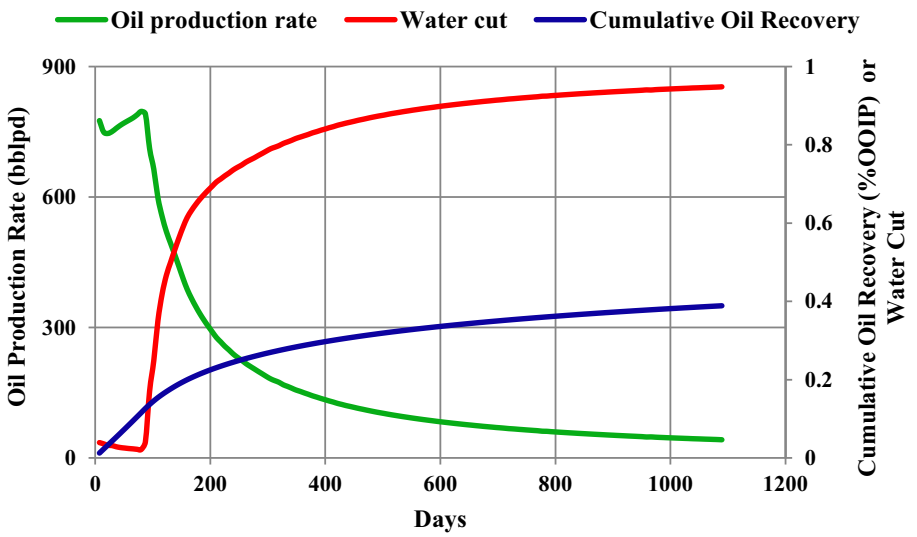

Fig. 22 Cumulative oil recovery, water cut and oil production rate during water flood

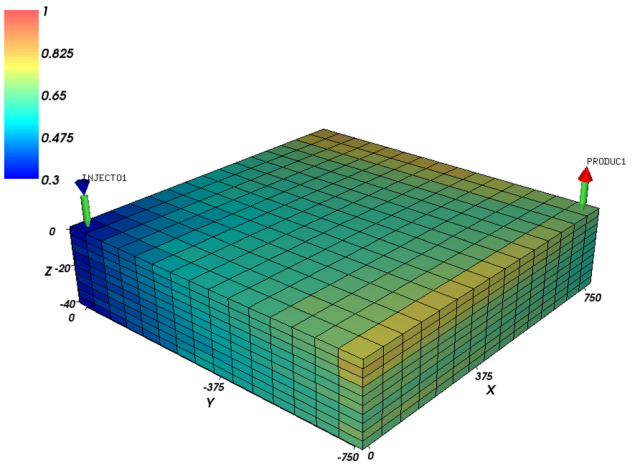

Fig. 23 Oil saturation distribution at the end of water flood

tional water flood. In the case of HPAM flood, cumulative oil recovery is about 36 % of residual oil in-place (ROIP) indicating the effectiveness of HPAM solution to enhance heavy oil recovery. Additionally, oil recovery further increases when the PAM solution has 0.9 wt% clay nanoparticles and ultimate oil recovery is around 40 % of ROIP. Moreover, 10 % increase (compared to HPAM flood) in the oil recovery is observed when dispersed silica nanoparticles in PAM solution are injected into the formation.

Figure 25 shows the overall water cut for three different injection scenarios. Based on the simulation results, production well is producing more water when the HPAM solution is an injectant. In addition, during DCNP flood the amount of water cut decreases and the efficiency of oil production improves. More importantly, during DSNP flood the amount of water cut also decreases and for more than 350 days the production well produces with water cut of less than 0.2. These results indicate that DSNP flood can further improve both cumulative oil recovery and water cut compared to both DCNP and HPAM floods.

Figure 26 shows the oil production rate versus injection days for HPAM, DCNP and DSNP floods. Both dispersed clay nanoparticles and dispersed silica nanoparticles can improve the oil production rate during both DCNP and DSNP floods compared to HPAM flood. In other words, oil will be produced faster when silica or clay nanoparticles are dispersed in injectant. Based on the simulation results, oil production rate increased after 350 injection days of HPAM, DCNP and DSNP floods. According to the results depicted in Fig. 26, oil production rate is equal to 208 barrels per day after 500 days of HPAM flood, while the amount of oil production rate, at the same injection time, is 281 barrels per days for DCNP flood. The oil production rate reduces sharply before 1000 days of injection for both HPAM and DCNP floods. For the case of DSNP flood, oil production rate increases to 331 barrels per day rapidly and it descends slowly compared

Table 7 Different injection designs

HPAM flood		DCNP flood		DSNP flood	
Slug size	1 PV	Slug size	1 PV	Slug size	1 PV
Polymer	1500 ppm HPAM	Polymer	1500 ppm, PAM	Polymer	1500 ppm, PAM
Concentration		Concentration		Concentration	
Nanoparticles concentration	–	Nanoparticles concentration	0.9 wt%	Nanoparticles concentration	0.45 wt%
Salinity	13,723 ppm	Salinity	13,723 ppm	Salinity	13,723 ppm
Injection rate	400 bbl/d	Injection rate	400 bbl/d	Injection rate	400 bbl/d
Post-water flood		Post-water flood		Post-water flood	
Injection time	0.5	Injection time	0.5	Injection time	0.5
Salinity	13,744 ppm	Salinity	13,744 ppm	Salinity	13,744 ppm
Injection rate	400 bbl/d	Injection rate	400 bbl/d	Injection rate	400 bbl/d

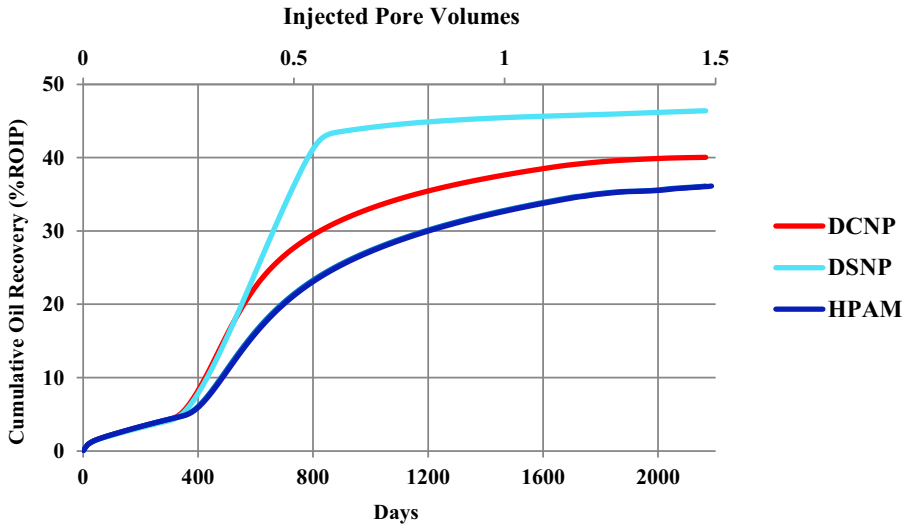

Fig. 24 Comparison of cumulative oil recovery for 3D simulations of HPAM flood, DCNP flood and DSNP flood

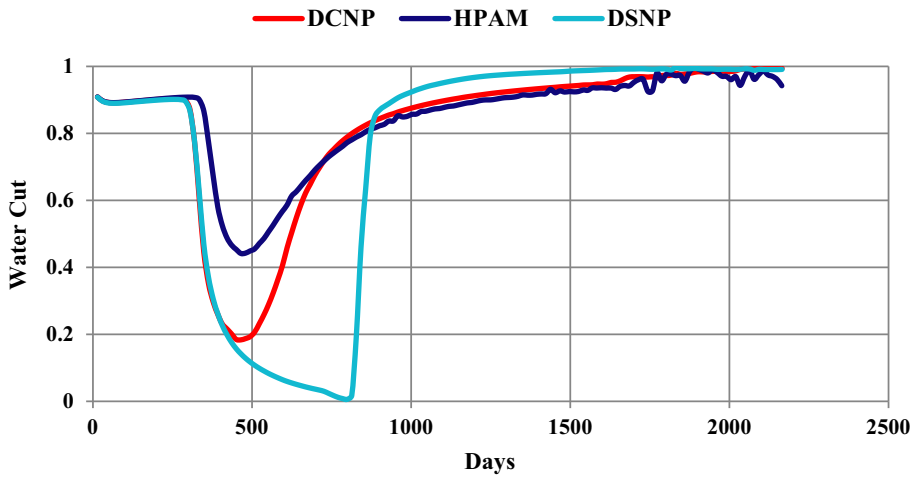

Fig. 25 Comparison of water cut for 3D simulations of HPAM flood, DCNP flood and DSNP flood

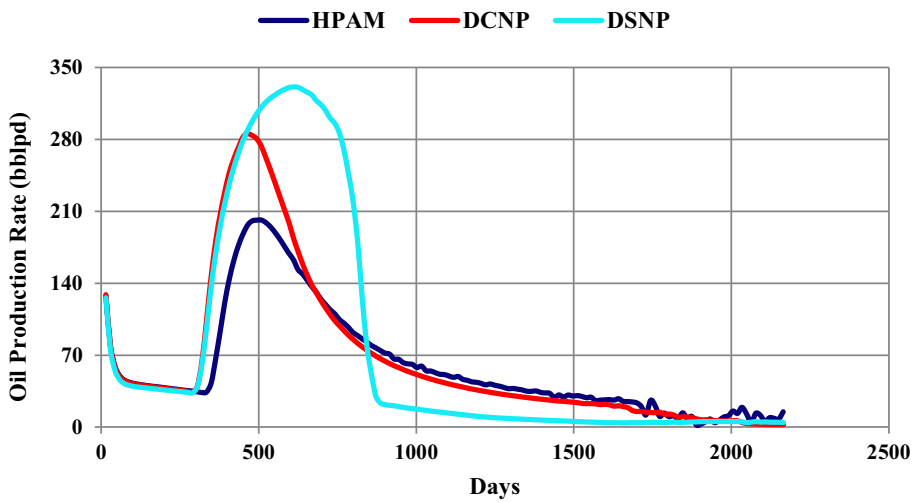

Fig. 26 Comparison of oil production rate for 3D simulations of HPAM flood, DCNP flood and DSNP flood

Table 8 Average oil saturation in each layer after water flood, HPAM flood, DCNP flood and DSNP flood

Numerical layer	$\bar{K}_X$ (md)	Average So_r after water flood	Average So_r after HPAM flood	Average So_r after DCNP flood	Average So_r after DSNP flood
1	2190	0.6285	0.4430	0.4220	0.3316
2	2620	0.5933	0.4135	0.3921	0.3204
3	2960	0.5816	0.3908	0.3797	0.3107
4	3680	0.55	0.3655	0.3610	0.3038
5	3680	0.5419	0.3664	0.3599	0.3028
6	3440	0.5460	0.3692	0.3617	0.3045
7	4120	0.5431	0.3655	0.3583	0.3006
8	3800	0.5416	0.3681	0.3623	0.3037
9	3220	0.5480	0.3765	0.3679	0.3088
10	3100	0.5387	0.3725	0.3651	0.3089

Table 9 Average oil recovery for each layer after HPAM flood, DCNP flood and DSNP flood

Numerical layer	Average oil recovery (%ROIP) after HPAM Flood	Average oil recovery (%ROIP) after DCNP flood	Average oil recovery (%ROIP) after DSNP flood
1	29.5	32.8	47.2
2	30.3	33.9	45.9
3	32.8	34.7	46.5
4	33.5	34.3	44.7
5	32.3	33.5	44.1
6	32.3	33.7	44.2
7	32.7	34	44.6
8	32.5	33.6	44.3
9	31.2	32.8	43.6
10	30.8	32.2	42.6

with other cases. Considering the experimental and numerical results about the effect of dispersed clay nanoparticles or dispersed silica nanoparticles on the polymer adsorption and solution viscosity, the DSNP flood makes a good sweep efficiency of untouched zone by other EOR options investigated in this paper. Consequently, oil production rate and cumulative oil recovery are much higher than HPAM and DCNP floods even in this viscous oil reservoir.

Table 8 gives the average residual oil saturation in each layer after HPAM, DCNP and DSNP floods. Moreover, average permeability in x-direction for each layer was calculated and presented in this table. Table 9 also shows the ultimate oil recovery in terms of %ROIP in each layer. Regarding these data, the effect of each injectant is investigated separately. Table 8 shows that the permeabilities of bottom layers are relatively higher than top layers. As a result of this relatively permeability contrast, a high-permeability path was created in the bottom where most of the injectant flow only through these layers during water flood and also even HPAM flood. Consequently, the amount of residual oil saturation of the bottom layers is relatively lower than that of top layers.

The amount of average oil saturation after DCNP and DSNP floods confirmed that injection of DSNP solution provides a favorable sweep efficiency for both low and high permeable layers. Accordingly, sweep efficiencies of the reservoir are more homogenous and ultimate oil recovery is high. In other words, DSNP solution reduces the negative effects of high heterogeneity and unfavorable mobility ratio on the overall oil recovery and oil recovery of each layer. As a result, the amount of residual oil saturation after DSNP flood is relatively low for all layers. Furthermore, injection of DCNP solution improves the ultimate oil recovery relatively compared to the HPAM flood. According to the simulation results presented in Table 9, the ultimate oil recovery is higher for DSNP flood compared with two other cases.

Figure 27 compares the amount of oil saturation at initial condition, after water flood, after HPAM flood, after DCNP flood and after DSNP flood for the second layer. The average permeability of this layer was about 2620 md which is considered as a low permeable layer compared to the other layers. So, this layer was selected to investigate the effect of water, HPAM, DCNP and DSNP floods on the residual oil saturation of the layer. According to the results, due to the permeability contrast and unfavorable mobility ratio, injectant did not penetrate to this layer considerably and the amount of oil saturation after water flood did not decrease remarkably compared to the initial oil saturation of this layer. By decreasing the mobility of water, the sweep efficiency improves during HPAM flood, but the negative effect of heterogeneity still prevents reduction in oil saturation of this layer. In addition, the amount of oil saturation dramatically decreased after both DCNP and DSNP floods.

Figure 28 compares the amount of cumulative oil recovery as a function of injection time for continuous water, HPAM, DCNP and DSNP floods. This figure shows that after 3255 days of water injection, the ultimate oil recovery factor in terms of %OOIP is about 44.6 %. In addition, the graph depicts that water injection is efficient until 1200 days. After that, water injection can increase cumulative oil recovery only 3 % because the amount of water cut increases and oil production rate decreases as the water injection continues. According to the results depicted in Fig. 28, HPAM, DCNP and DSNP floods improve the cumulative oil recovery after 1090 days of water injection. However, DSNP flood has a positive strong effect on oil recovery compared to the other cases. Moreover, DCNP flood is more useful than HPAM flood in terms of improvement in oil recovery.

5 Conclusion and Recommendations

The main findings of this work and some recommendations for further study can be summarized as follows:

1. A series of experiments to study the impact of silica nanoparticles and clay nanoparticles on the rheological properties of PAM solution were carried out. Experimental observations showed that silica nanoparticles can increase the amount of solution viscosity and decrease the amount of polymer adsorption onto the rock remarkably. Clay nanoparticles also increase the solution viscosity and decrease the amount of polymer adsorption onto the rock surface, but with a lesser extent compared to the silica nanoparticles. These unique features of silica and clay nanoparticles are useful in improvement of polymer solution properties in CEOR applications.
2. According to the properties of prepared solutions, UTCHEM parameters needed to simulate DCNP and DSNP floods were calculated. In other words, input parameters for simulation of DCNP and DSNP floods were successfully matched by the use of UTCHEM polymer models and experimental data. To the extent of our knowledge, this is the first time that the properties of dispersed nanoparticles in polymer solution are matched with chemical compositional simulator polymer models to simulate DNP floods.
3. Based on the experimental results of the recently published HPAM core flood, 1D simulation model was constructed and history match of oil saturation data between simulation model and experimental results was carried out. The validated simulation model was used to simulate both DCNP and DSNP floods. The simulation results showed that cumulative heavy oil recovery is higher for DSNP and DCNP floods compared to HPAM flood. Moreover, aqueous viscosity profile and the amount of

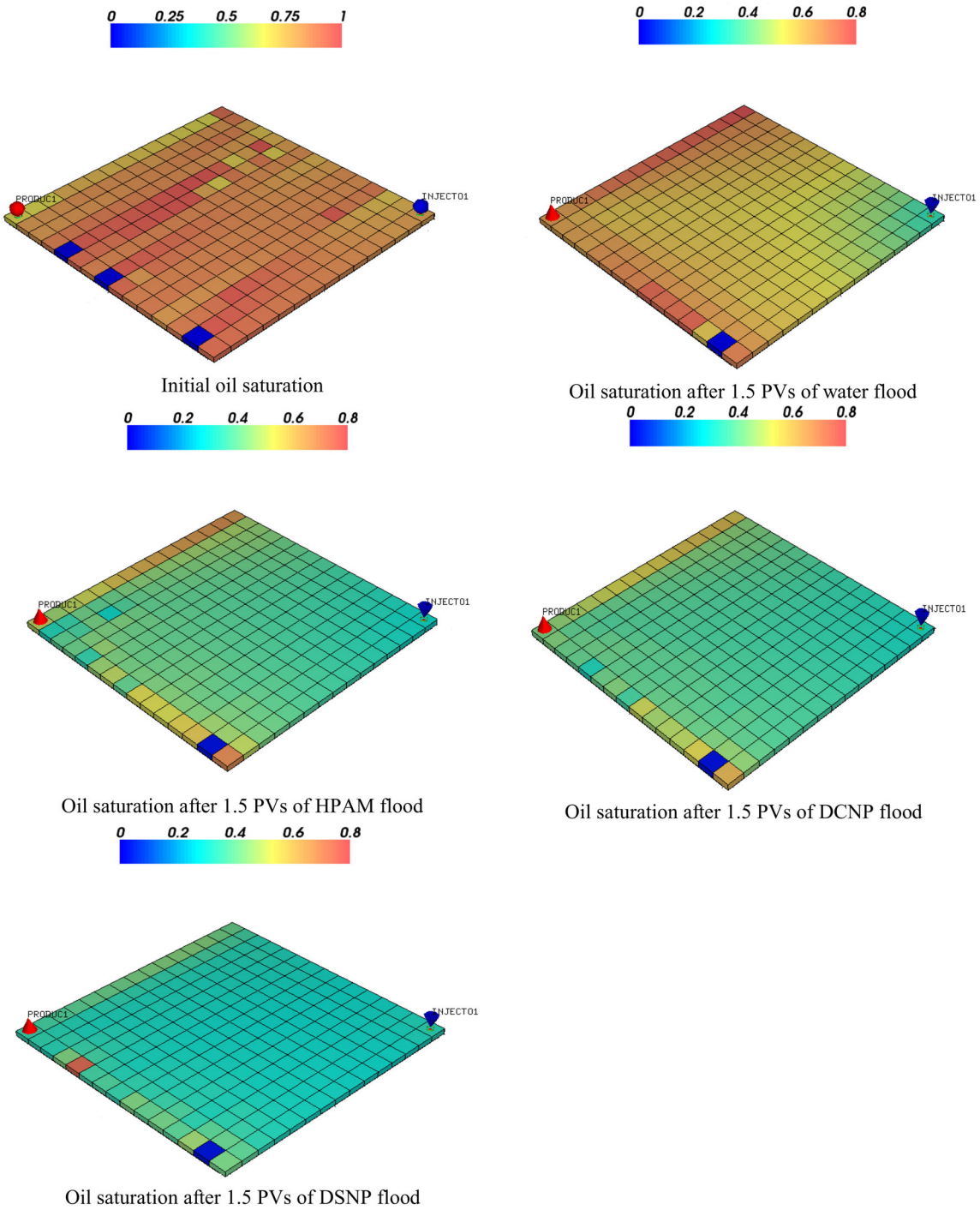

Fig. 27 Distribution of oil saturation at the second layer

polymer adsorption during DSNP or DCNP floods are more favorable to recover heavy oil.

4. 3D simulations of DCNP and DSNP floods for a highly heterogeneous reservoir showed that these solutions can improve oil recovery in such reservoirs, especially in low permeable layers. The simulation results demonstrated that improved rheological properties of PAM solution by the use of nanoparticles can strongly affect the performance of PAM solution for heavy oil recovery.
5. In this paper, the effect of silica and clay nanoparticles on wettability alteration of rock was not considered; however, some researchers [25,35] and [36] showed that dispersed nanoparticles can be used as wettability modifiers. As a result, the effect of dispersed nanoparticles on

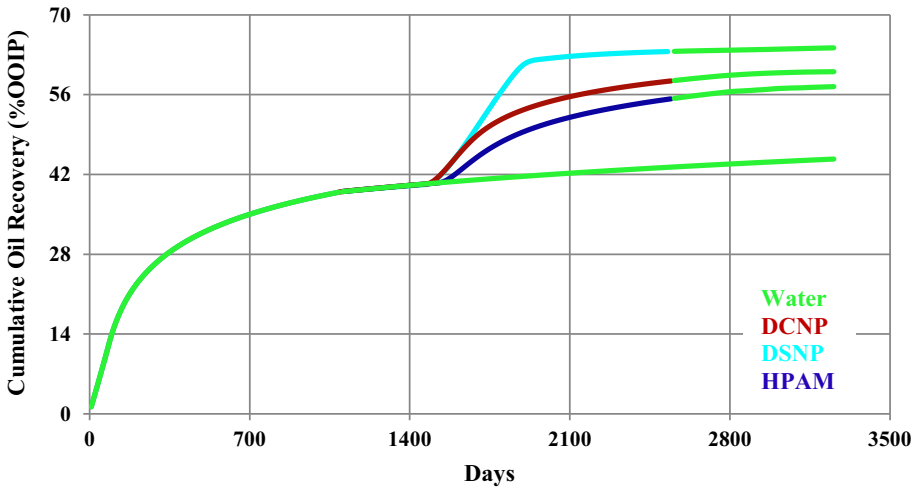

Fig. 28 Cumulative oil recovery versus injection time in terms of initial oil in-place

wettability alteration of rock should be modeled through the use of simulators which have the capability of modeling wettability alteration of reservoir rocks to understand the main mechanisms involved in NAP flood.

Acknowledgments The work was conducted with the financial support of Islamic Azad University of Quchan branch. The financial support from Iran Nanotechnology Initiative Council is also acknowledged. The authors are also grateful to National Iranian Oil Company and Khorasan Science and Technology Park for providing technical facilities. We would like to thank ESSS for providing the post-processor software needed to complete this research. The corresponding author also thanks Ms. Erfani for extensive review, her valuable comments and contribution for the improvements of this manuscript.

References

1. Mai, A.; Bryan, J.; Goodarzi, N.; Kantzas, A.: Insight into non-thermal recovery of heavy oil. J. Can. Pet. Technol. **48**, 27–35 (2009). doi:10.2118/09-03-27
2. Farouq, A.: Prospects of EOR techniques in Saskatchewan oil reservoirs. J. Can. Pet. Technol. **25**, 64–68 (1986). doi:10.2118/86-02-04
3. Foo, Y.Y.; Chee, S.C.; Md. Zain, Z.; Mamora, D.D.: Recovery processes of extra heavy oil-mechanistic modeling and simulation approach. In: Paper SPE 143390 (2011). doi:10.2118/143390-MS
4. Bondino, I.; Santanach-Carreras, E.; Levitt, D.; Jouenne, S.; Bourrel, M.: Polymer flooding of heavy oil under adverse mobility conditions. In: Paper SPE 165267 (2013). doi:10.2118/165267-MS
5. Shamekhi, H.; Kantzas, A.; Bryan, J.; Su, S.: Insights into heavy oil recovery by surfactant, polymer and ASP flooding. In: Paper SPE 165440 (2013). doi:10.2118/165440-MS
6. Van Heel, A.; Van Drop, J.; Boerrigter, P.M.: Heavy oil recovery by steam injection in fractured reservoirs. In: Paper SPE 113461 (2008). doi:10.2118/113461-MS
7. Buckles, R.S.: Steam stimulation heavy oil recovery at Cold Lake, Alberta. In: Paper SPE 7994 (1979). doi:10.2118/7994-MS
8. Farouq Ali, S.M.: Heavy oil recovery-principles, practicality, potential, and problems. In: Paper SPE 4935 (1974). doi:10.2118/4935-MS
9. Butler, R.M.; Mokrys, I.J.: A new process (VAPEX) for recovering heavy oil using hot water and hydrocarbon vapor. J. Can. Pet. Technol. **30** (1991). doi:10.2118/91-01-09
10. Shen, C.: Limitations and potentials of in-situ combustion processes for heavy oil reservoirs. In: Paper PETSOC-2002-217 (2002). doi:10.2118/2002-217
11. Center for Petroleum and Geosystems Engineering, The University of Texas at Austin (Producer), Chemical EOR-what's new, whats works, where to use it (2015). http://www.cpge.utexas.edu/?q=111115_eor
12. Kumar, R.; Mohanty, K.: Sweep efficiency of heavy oil recovery by chemical floods. In: Paper SPE 146839 (2011). doi:10.2118/146839-MS
13. Panthi, K.; Sharma, H.; Mohanty, K.K.: ASP flood of a viscous oil in a carbonate rock. Fuel **164**, 18–27 (2015). doi:10.1016/j.fuel.2015.09.072
14. Seright, R.S.: Potential of polymer flooding reservoirs with viscous oils. SPE Reserv. Eval. Eng. **13**, 730–740 (2010). doi:10.2118/129899-PA
15. Aitkulov, A.: Two-dimensional ASP flood of viscous oil (MS Thesis), The University of Texas at Austin, Austin, Texas (2014)
16. Fortenberry, R.: Experimental demonstration and improvement of chemical EOR techniques in heavy oils (MS Thesis), The University of Texas at Austin, Austin, Texas (2013)
17. Fortenberry, R.; Suniga, P.; Mothersele, S.; Delshad, M.; Lashgari, H.; Pope, G.A.: Selection of chemical EOR strategy in a heavy oil reservoir using laboratory data and reservoir simulation. In: Paper SPE 174520 (2015). doi:10.2118/174520-MS
18. Needham, R.; Doe, P.: Polymer flooding review. J. Pet. Technol. **39**, 1503–1507 (1987). doi:10.2118/17140-PA
19. Sheng, J.; Leonhardt, B.; Azri, N.: Status of polymer-flooding technology. J. Can. Pet. Technol. **54**, 116–126 (2015). doi:10.2118/174541-PA
20. Gogarty, W.B.: Mobility control with polymer solutions. SPE J. **7**, 161–173 (1967). doi:10.2118/1566-B
21. Pu, H.; Yin, D.: Study of polymer flooding in class III reservoir and pilot test. In: Paper SPE 109546 (2008). doi:10.2118/109546-MS
22. Littman, W.: Polymer Flooding, No. 24. Developments in Petroleum Science, Elsevier Science Publishers B.V., Amsterdam (1988)
23. Kurenkov, V.F.; Harten, H.G.; Lobanov, F.I.: Degradation of polyacrylamide and its derivatives in aqueous solutions. Russ J Appl Chem **75**, 1039–1050 (2002). doi:10.1023/A:1020747523268
24. Caufield, M.J.; Hao, X.; Qiau, G.G.; Solomon, D.H.: Degradation on polyacrylamides: part II, polyacrylamide gels. J Polym **44**, 3817–3826 (2003). doi:10.1016/S0032-3861(03)00330-6
25. Aminnaji, M.; Fazeli, H.; Bahramian, A.; Gerami, S.; Ghojavand, H.: Wettability alteration of reservoir rocks from liquid wetting

to gas wetting using nanofluid. Transp. Porous Media **109**, 201–216 (2015). doi:10.1007/s11242-015-0509-6
26. Zargartalebi, M.; Kharrat, R.; Barati, N.: Enhancement of surfactant flooding performance by the use of silica nanoparticles. Fuel **143**, 21–27 (2015). doi:10.1016/j.fuel.2014.11.040
27. Khalilinezhad, S.S.; Cheraghian, G.: Mechanisms behind injecting the combination of nano-clay particles and polymer solution for enhanced oil recovery. Appl. Nanosci. (2015). doi:10.1007/s13204-015-0500-0
28. Zargartalebi, M.; Barati, N.; Kharrat, R.: Influences of hydrophilic silica nanoparticles on anionic surfactant properties: interfacial and adsorption behaviors. J. Pet. Sci. Eng. **119**, 36–43 (2014). doi:10.1016/j.petrol.2014.04.010
29. Alghamdi, A.A.L.: Experimental evaluation of nanoparticles impact on displacement dynamics for water-wet and oil-wet porous media. (MS Thesis), The University of Texas at Austin, Austin, Texas (2015)
30. Cheraghian, G.; Khalilinezhad, S.S.: Effect of nano clay on heavy oil recovery during polymer flooding. J. Pet. Sci. Technol. **33**, 999–1007 (2015). doi:10.1080/10916466.2015.1014962
31. Ahmad, Y.K.: Nano-particles-stabilized oil-in-water emulsions for residual oil recovery (MS Thesis), The University of Texas at Austin, Austin, Texas (2015)
32. Hendraningrat, L.; Li, S.; Torsaeter, O.: A core flood investigation of nanofluid enhanced oil recovery. J. Pet. Sci. Eng. **111**, 128–138 (2013). doi:10.1016/j.petrol.2013.07.003
33. Mohajeri, M.; Hemmati, M.; Shekarabi, A.Z.: An experimental study on using a nanosurfactant in an EOR process of heavy oil in a fractured micromodel. J. Pet. Sci. Eng. **126**, 162–173 (2015). doi:10.1016/j.petrol.2014.11.012
34. Maghzi, A.; Kharrat, R.; Mohebbi, A.; Ghazanfari, M.H.: The impact of silica nanoparticles on the performance of polymer solution in presence of salt in polymer flooding for heavy oil recovery. Fuel **123**, 123–132 (2014). doi:10.1016/j.fuel.2014.01.017
35. Maghzi, A.; Mohebbi, A.; Kharrat, R.; Ghazanfari, M.H.: Pore scale monitoring wettability alteration by silica nanoparticles during polymer flooding to heavy oil in a five-spot glass micromodels. Transp. Porous Media **87**, 653–664 (2010). doi:10.1007/s11242-010-9696-3
36. Maghzi, A.; Mohammadi, S.; Ghazanfari, M.H.; Kharrat, R.; Masihi, M.: Monitoring wettability alteration by silica nanoparticles during water flooding to heavy oils in a five-spot systems: a pore level investigation. Exp. Therm. Fluid Sci. **40**, 168–176 (2012). doi:10.1016/j.expthermflusci.2012.03.004
37. Saad, N.: Field scale simulation of chemical flooding, (Ph.D. Dissertation), The University of Texas at Austin, Austin, Texas (1989)
38. Bhuyan, D.: Development of an alkaline/surfactant/polymer compositional reservoir simulator, (Ph.D. Dissertation), The University of Texas at Austin, Austin, Texas (1989)
39. Delshad, M.; Pope, G.A.; Sepehrnoori, K.: A compositional simulator for modeling surfactant enhanced aquifer remediation, 1 formulation. J. Contam. Hydrol. **23**, 303–327 (1996). doi:10.1016/0169-7722(95)00106-9
40. UTCHEM-9.0, A three-dimensional chemical flood simulator, Volumes 1 and 2, Reservoir Engineering Research Program, Center for Petroleum and Geosystems Engineering, The University of Texas at Austin (2000)
41. Saad, N.; Pope, G.A.; Sepehrnoori, K.: Simulation of big muddy surfactant pilot. SPE Reserv. Eng. **4**, 24–34 (1989). doi:10.2118/17549-PA
42. Takagi, S.: Field-scale simulation of chateaurenard polymer pilot (MS Thesis), The University of Texas at Austin, Austin, Texas (1992)
43. Goudarzi, A.: Modeling conformance control and chemical EOR processes using different reservoir simulators (Ph.D. Dissertation), The University of Texas at Austin, Austin, Texas (2015)
44. Korrani, A.K.N.; Sepehrnoori, K.; Delshad, M.: A mechanistic integrated geochemical and chemical-flooding tool for alkaline-surfactant-polymer floods. SPE J. **21**, 32–54 (2016). doi:10.2118/169094-PA
45. Donaldson, E.C.; Chilingarian, G.V.; Yen, T.F.: Enhanced oil recovery. II processes and operations. Elsevier Science Publishers B.V, Amsterdam (1989)
46. Brookfield DV-III Ultra, A Programmable Rheometer, Manual Number: M/98-211-E0912, Brookfield Engineering Laboratories Inc. USA. http://www.brookfieldengineering.com/download/files/DVIIIUltraC.pdf
47. Cheraghian, G.; Khalilinezhad, S.S.; Kamari, M.; Hemmati, M.; Masihi, M.; Bazgir, S.: Adsorption polymer on reservoir rocks and role of the nano-particles, clay and silica. J. Int. Nano Lett. **4**, 114–121 (2014). doi:10.1007/s40089-014-0114-7
48. Ehrenfried, D.H.: Impact of viscoelastic polymer flooding on residual oil saturation in sandstones (MS Thesis), The University of Texas at Austin, Austin, Texas (2013)
49. Mohammadi, H.: Mechanistic modeling, design, and optimization of alkaline/surfactant/polymer flooding (Ph.D. Dissertation), The University of Texas at Austin, Austin, Texas (2008)
50. Zhao, F.-L.: Chemistry in Oil Production. University of Petroleum, China (1991)
51. Sheng, J.J.: Modern chemical enhanced oil recovery: theory and practice. Elsevier, Amsterdam (2011) . doi:10.1016/B978-1-85617-745-0.00005-X
52. Chiappa, L.; Mennella, A.; Lockart, T.P.; Burrafato, G.: Polymer adsorption at the brine/rock interface: the role of electrostatic and wettability. J. Pet. Sci. Eng. **24**, 113–122 (1999). doi:10.1016/S0920-4105(99)00035-2
53. Skauge, T.; Spildo, K.; Skauge, A.: Nano-sized particles for EOR. In: Paper SPE 129933 (2008). doi:10.2118/129933-MS
54. Kazempour, M.; Sundstrom, E.A.; Alvarado, V.: Effect of alkalinity on oil recovery during polymer floods in sandstones. SPE J. **15**, 195–209 (2012). doi:10.2118/141331-PA
55. Cheraghian, G.; Nezhad, S.S.K.; Bazgir, S.: Improvement of thermal stability of polyacrylamide solution used as a nano-fluid in enhanced oil recovery process by nano clay. Int. J. Nanosci. Nanotechnol. **11**, 201–208 (2015)